Powder Technology 246 (2013) 63–72

Contents lists available at SciVerse ScienceDirect

Powder Technology

journal homepage: www.elsevier.com/locate/powtec

Effects of powder flow properties and shear environment on the performance of continuous mixing of pharmaceutical powders

Aditya U. Vanarase, Juan G. Osorio, Fernando J. Muzzio *

Department of Chemical and Biochemical Engineering, Rutgers, The State University of New Jersey, Piscataway, NJ 08854, United States

ARTICLE INFO

Article history:
Received 11 August 2012
Received in revised form 30 April 2013
Accepted 2 May 2013
Available online 9 May 2013

Keywords:
Continuous powder mixing
RTD (Residence Time Distribution)
High-shear mixing
PLS model

ABSTRACT

This paper focuses on two aspects of continuous powder mixing, namely characterizing the effects of material properties on the bulk powder flow behavior, and developing continuous blending strategies suitable for cohesive materials. The relative effects of process parameters and material properties on the bulk powder flow behavior were analyzed by performing a PLS analysis of the output parameters, including mean residence time, and axial dispersion coefficient as a function of input parameters (impeller speed, flow rate, bulk density and cohesion). The mean residence time was primarily affected by the bulk density and impeller speed, whereas the axial dispersion coefficient was affected by impeller speed and cohesion. Based on previously developed knowledge of mixing performance as a function of process parameters [1], a design rule to select the optimal number of impeller passes based on the bulk density was proposed. Impeller speed and cohesion showed a significant interacting effect on the output variable, the axial dispersion coefficient. Increase in cohesion leads to increase in the axial dispersion coefficient at higher impeller speeds, whereas a negligible effect of cohesion on the axial dispersion coefficient was observed at lower impeller speeds. In the second part of the paper, a continuous blending methodology for blending cohesive materials was demonstrated. Considering the feeding limitations of cohesive materials, and limitations in the application of shear in the bladed continuous mixer, a combination of high shear and low shear mixing with high-shear mixing as a first step exhibited an optimal mixing strategy.

1. Introduction

There are typically five routes for manufacturing solid dose pharmaceutical products, namely direct compression, dry granulation, wet granulation, capsule filling and hot-melt extrusion. Powder mixing is an essential process in all the aforementioned manufacturing routes. Since pharmaceutical processes are conventionally carried out in the batch mode, the available knowledge for the mixing of pharmaceutical powders pertains to batch processes and the necessary methods or design rules required to develop an equivalent continuous process are scarce within the literature. This paper focuses on two aspects of continuous powder mixing — developing a relationship between bulk material properties and the flow behavior in continuous mixing systems, and developing an integrated low and high shear continuous mixing processes suitable for mixing highly cohesive powders.

In recent years there have been quite a few papers published in the literature focusing on the characterization of continuous powder blending processes using either purely experimental approaches [1–4], or using computational modeling approaches such as the Discrete Element Method (DEM) [5]. In both approaches, typically the observed mixing behavior is related to the powder flow behavior in the mixer. In the DEM modeling approach, powder flow behavior is characterized by computing the velocity probability density functions (PDFs) and/or dispersion coefficients, whereas in the experimental approach PIV (Particle Image Velocimetry) or RTD (Residence Time Distribution) measurements are performed. The RTD approach is interesting because it can be used to build predictive models which predict powder concentration at the blender discharge as a function of incoming concentrations [6] and process parameters, which essentially makes it suitable for process control. In the literature, Fokker Plank Equations (FPEs) [7,8] have been widely used to model RTDs since the number of fitted parameters in the FPE is small compared to other modeling approaches such as Markov chains [9], tanks-in-series, or fractional tubularity models [10].

In our previous paper [11], FPEs were used to model RTDs from the Gericke GCM-250 mixer, and a mathematical model was developed to relate mixing performance with the incoming feed rate variability and process parameters (blender speed, flow rate). Typically such models are valid for a particular formulation and they are

* Corresponding author at: Department of Chemical and Biochemical Engineering, Rutgers University, 98 Brett Road, Piscataway, NJ 08854, United States.
E-mail addresses: doug.hausner@gmail.com, fjmuzzio@yahoo.com (F.J. Muzzio).

0032-5910
http://dx.doi.org/10.1016/j.powtec.2013.05.002

difficult to transfer for completely new formulations without prior experimental studies. The missing link in this case is the relationship between material properties and RTDs. In this paper, key material properties of commonly used pharmaceutical excipients were identified and correlated with the RTD parameters. The approach typically involves the measurement of RTD and fitting the model parameters such as the mean residence time and the axial dispersion coefficient.

The second part of this paper focuses on the development of alternative continuous mixing strategies for materials which tend to form agglomerates in powder blends. APIs (Active Pharmaceutical Ingredients) that have an average size of less than 20 μm in diameter are highly cohesive, and tend to form agglomerates because of the overwhelming Van der Waals forces. Cohesion in powder/granular systems is also caused by the capillary forces that exist due to the presence of moisture in the system; however in the present case of dry powders the primary source of cohesion is Van der Waals forces and/or electrostatic forces [12]. Powders that tend to agglomerate are typically mixed in a high shear rate environment such that the agglomerates are de-lumped and an, sometimes, an "ordered mixture" is created. High shear blending is typically performed using a V-blender with a high-speed intensifier bar, a convective mixer with a chopper, or by introducing a mill [13]. In this study, a Comil was selected as a suitable continuous de-lumping device. In order to qualify the feasibility of a Comil for the continuous process, its efficiency for mixing and de-lumping needs to be examined. In this paper, the effect of Comil process parameters on mixing performance and its position in the overall continuous processing scheme is examined.

This paper is organized as follows. In the second section, materials and methods are presented. In the third section, equipment used in this study is described. The fourth section focuses on results, which include the characterization of effects of material properties on RTD parameters, and the integrated design of mixing and de-lumping. Finally, conclusions are presented in the fifth section.

2. Materials and methods

2.1. Materials

The materials used in this study, their mean particle size and the supplier are listed in Table 1. In the first part of the paper, excipients including micro-crystalline cellulose (Avicel® PH-200, Avicel® PH-101), Fast Flo lactose, and dicalcium phosphate were used as the model materials to study the effect of material properties on the powder flow behavior in the mixer. Acetaminophen was used as a tracer material for measuring RTDs for micro-crystalline cellulose and lactose, whereas caffeine was used as a tracer for dicalcium phosphate. In the second part of this paper, Avicel® PH-200 was used as the model free-flowing powder and acetaminophen (micronized) was used as the model cohesive drug.

Table 1
Materials.

Material	Supplier	Particle size (μm) (d50)
Avicel® PH-200	FMC Biopolymer	230
Avicel® PH-101	FMC Biopolymer	90
Fast Flo lactose	Foremost Farms USA	120
Dicalcium phosphate	TLC Ingredients	186
Acetaminophen (APAP) (micronized)	Mallinckrodt	20
Caffeine	TLC Ingredients	36

2.2. Methods

2.2.1. NIR spectroscopy

Chemical composition of the powder samples were analyzed using NIR spectroscopy. Chemometric calibration models were built for individual tracer-excipient combinations. The general protocol for building calibration models includes the following steps. Calibration samples with known concentrations of tracer are prepared by accurately massing the individual components. Calibration samples are then scanned multiple times to acquire representative spectra. The NIR analyzer used was an Antaris system (Thermo Fisher). The Ominc software package was used to acquire the calibration spectra, and the TQ Analyst was used to build the chemometric model. A PLS algorithm was used to build calibration curves. Each calibration model was validated using a cross-validation program (which leaves one spectra out at a time); in each case, after careful selection of spectral pre-treatments, a robust calibration model was built. The calibration model used in the second part of this study for measuring APAP in APAP-Avicel® PH-200 mixtures is shown in Fig. 1. The calibration error (RMSEP) for this model was ~0.44.

2.2.2. Material properties

Material flow properties were characterized using two methods, namely the Carr Index (C.I.) and the dilation.

2.2.2.1. Carr Index. The Carr Index (C.I.) is an indicator of the compressibility of a powder. The higher the C.I. is, more compressible is the powder. The C.I. was calculated using Eq. (1) by measuring the bulk and tapped densities of a powder. C.I. measurements are listed in Table 2.

$$\text{C.I.} = 100 \times \left(1 - \frac{\rho_B}{\rho_T}\right) \tag{1}$$

2.2.2.2. Dilation. Dilation is a complementary measurement to the C.I. which is also an indicator of the compressibility of the powder. Dilation was measured using a device called a GDR (Gravitational Displacement Rheometer). Dilation is calculated as the percent change in volume of the powder bed as function of time. Details on the experimental set-up of dilation measurement can be found in Faqih et al. [14]. The procedure for dilation measurement can be briefly described as follows. Powder was filled up to 40% volume in a transparent acrylic cylinder, and then the cylinder was tapped on a tapping machine such that powder is compacted to its tapped density. The cylinder was then mounted on the GDR, which rotates the cylinder such that the powder tumbles inside the cylinder. The tumbling or avalanching motion of the powder is monitored in the cross-sectional direction using a camera. The images being captured using the camera are subsequently analyzed using an image analysis program to measure the

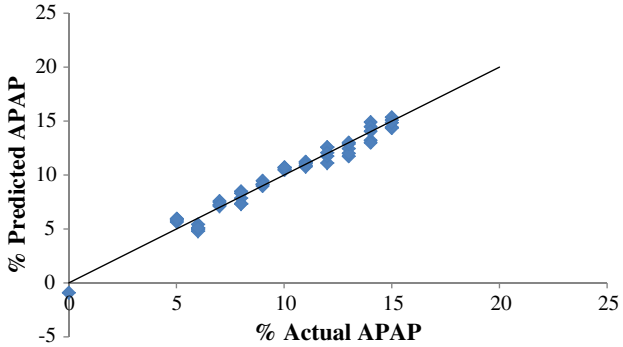

Fig. 1. Calibration model for APAP-Avicel® PH-200 mixture.

Table 2
Bulk density, Carr Index, dilation, particle size of excipients.

Material	Bulk density (g/cm^3)	Carr Index (C.I.)	% dilation	d50 (μm)
Avicel® PH-101	0.33	22.25	48.67	90
Avicel® PH-200	0.38	10.97	16.2	230
Fast Flo lactose	0.59	9.67	22.05	120
Dicalcium phosphate ($CaHPO_4$)	0.77	15.27	29.47	186

change in the cross sectional area of the powder. By making an assumption of uniform cross sectional area across the length of the cylinder, powder dilation can be calculated.

The dilation measurement, although complementary to the C.I., is more accurate, both because it is measured under the fully dilated state of the powder and because the common errors involved in bulk density measurements, such as powder compaction while filling the cylinder or inaccurate volume measurement due to an uneven powder surface, can be avoided in this measurement. Dilation is an indicator of the level of cohesion present in a powder; the greater the dilation, the more cohesive the powder. This fact has been proved for several materials through experimental as well as computational studies [14]. Thus in our experimental studies dilation was used as the material property that represents cohesion in the system. Dilation values of the materials used our study are listed in Table 2.

2.2.2.3. Bulk density. Bulk density was used as the second bulk material property in this study. Bulk density measurements were performed by pouring powder in a graduated cylinder, and recording the mass and volume of the powder. Bulk density values for the excipients are listed in Table 2.

3. Equipment

3.1. Continuous powder mixer — Gericke GCM-250

A continuous powder mixer supplied by Gericke (GCM-250) (Fig. 2(a)) was used in this study. The mixer consists of a stationary horizontal shell with an impeller rotating along its axis. The impeller (Fig. 2(b)) design consists of 12 triangular shaped blades mounted on its axis in a spiral fashion.

3.2. Conical mill — Quadro-197

A conical mill (Comil) manufactured by Quadro (Model # 197) (Fig. 3) was utilized in this study. Since the mill was used for de-lumping purposes and not size reduction, it was operated using a round impeller (Model # 1601), and screens with round holes, which apply less shear on the material. The screen diameter was selected such that stagnation of the material in the mill was minimal, and hence particle breakage avoided. Screens with large diameter are not recommended since their efficiency for de-lumping is less than desirable. Screens with hole diameters of 600 and 800 μm were used in this study, which provided adequate de-lumping efficiency, as demonstrated by the lack of agglomerates in the blend.

3.3. Gravimetric feeders

Gravimetric feeders supplied by Schenck Accurate (Model — Pure Feed) were used to feed powders in the continuous mixer or in the mill. Optimal combination of nozzle size and screw type was selected to feed each powder. The screw designs used for feeding powders are shown in Fig. 4. Typically a 2″ nozzle and a helical screw with the center-shaft were used to feed all the excipients. It was difficult to feed micronized acetaminophen using the helical screw with the center-shaft because of the lesser filling of Acetaminophen in each screw rotation. Since Acetaminophen is highly cohesive, higher volume per revolution is necessary in order to obtain the required throughput. A screw with open helix satisfied the necessary throughput requirement and was thus used to feed micronized acetaminophen.

4. Results

Results are presented in two sub-sections. The first section focuses on the characterization of powder flow behavior in the mixer for different excipients.

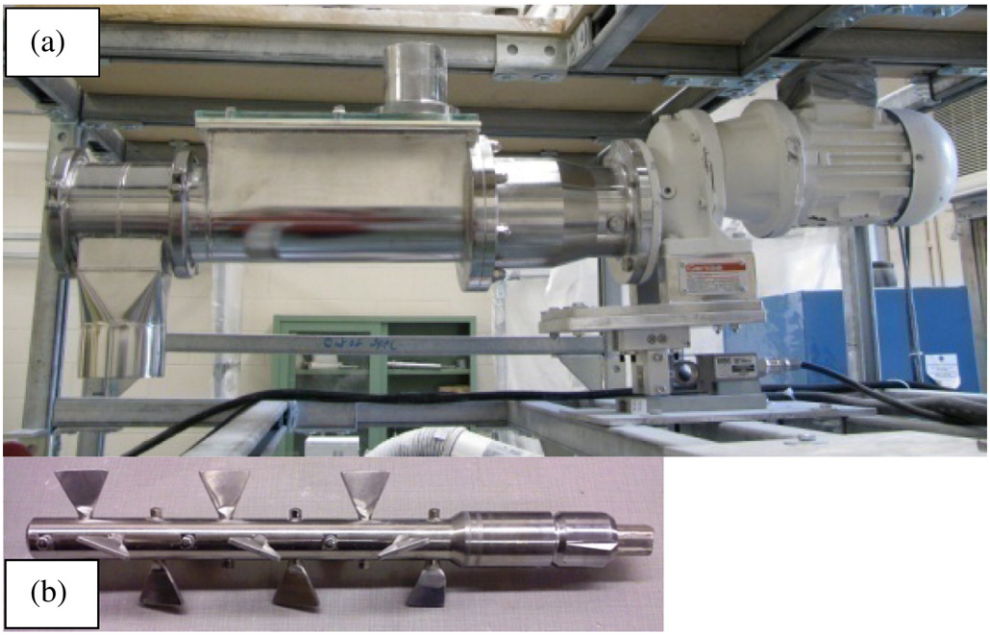

Fig. 2. (a) Continuous powder mixer (Gericke GCM-250). (b) Impeller design.

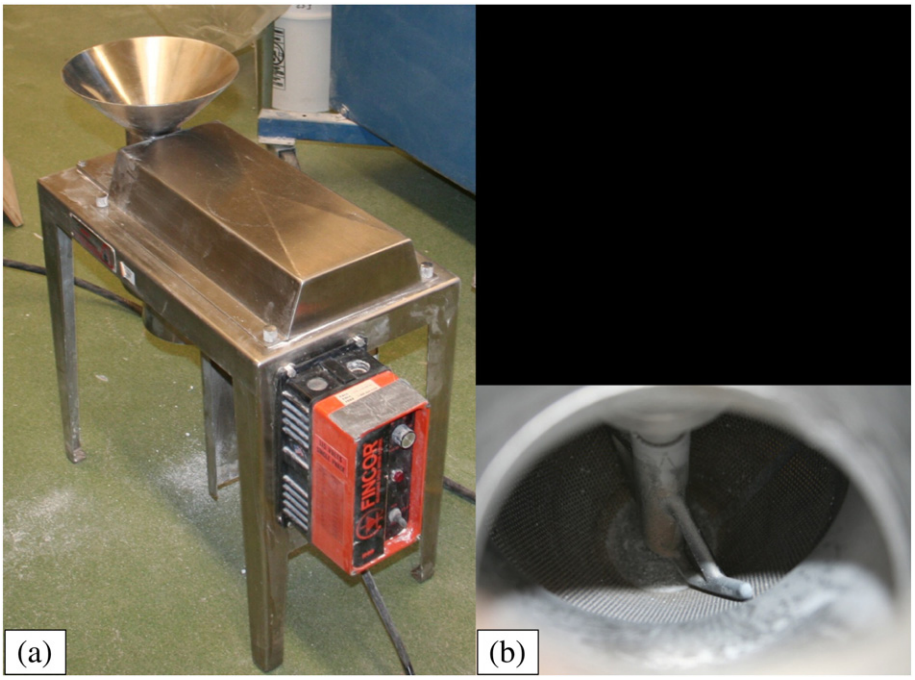

Fig. 3. (a) Conical mill (Quadro Model # 197). (b) Milling chamber with conical round impeller.

4.1. Effects of bulk material properties on the flow behavior in the continuous mixer

RTDs in continuous mixers are dependent on the mixer geometry, impeller speed, flow rate and material properties of the powder. In our previous publication [1], relationships between RTD and process (flow rate, impeller speed) and design parameters (impeller design, weir angle) were reported. In this paper, the original parametric space of process parameters (flow rate, impeller speed) was extended to include different materials. The materials used in this DoEs (Design of Experiments) are presented in Table 2. Essentially two bulk material properties (bulk density and cohesion) were correlated with the observed RTD parameters.

4.1.1. Methodology for RTD measurement and axial dispersion model fitting

RTD measurements were conducted by introducing a "pulse" of a suitable tracer into the mixer and measuring the tracer concentration at the blender discharge as a function of time. Tracer amounts were selected such that the concentration of the tracer at the mixer discharge was detectable using NIR spectroscopy and it was within the range of the calibration curve. RTD data was fitted using the axial dispersion model given in Eq. (2). In Eq. (2), θ is the dimensionless residence time and ξ is the dimensionless location in the continuous mixer. t_0 represents the time delay in the RTD measurement, τ is the mean residence time and L is the overall length of the continuous mixer. In Eq. (2), when $\xi = 1$, it represents the RTD of the continuous mixer. Fitting parameters in Eq. (2) are residence time (τ), time delay (t_0), and the Peclet number (Pe). C_0 is the pulse strength, calculated using the tracer amount provided in the RTD experiment. Once the parameters are estimated, the total residence time ($\tau_{Total} = \tau + t_0$) and axial dispersion coefficient (D_z) can be calculated. The methodology used for model fitting is described in detail in Gao et al. [11].

$$C(\xi,\theta) = \frac{C_0}{2\sqrt{\pi\theta/Pe}} \exp\left[\frac{-(\xi-\theta)^2}{4\theta/Pe}\right] \quad (2)$$

$$\theta = \frac{t-t_0}{\tau}, \xi = \frac{l}{L}, D_z = \frac{L^2}{\tau.Pe}$$

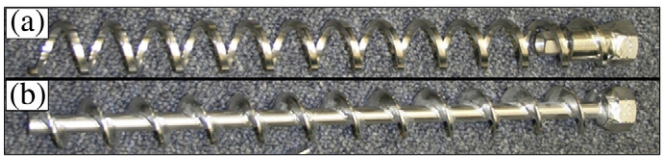

Fig. 4. Screw designs. (a) Open helical screw. (b) Helical screw with center shaft.

4.1.2. Effect of material properties on the mean residence time

In our previous publication [1] it was shown that the residence time is a strong function of impeller speed. Flow rate also affects residence time, but it displays an interaction with the impeller speed. At lower impeller speeds, higher flow rates show lower residence times, whereas at higher impeller speeds, the effect of the flow rate becomes negligible. In this DoE, a PLS analysis was performed on the dataset consisting of an output variable (mean residence time) and four input variables (impeller speed, flow rate, bulk density and cohesion). The PLS analysis was performed using a multi-variate data analysis software program, 'ProSensus Multivariate'. In the PLS analysis, 85% of the total variance was captured using just the first principal component (Fig. 5). Addition of another principle component did not increase the R^2 value of the model. The relative trends between all the input and output variables are presented using a loading plot in Fig. 6. The mean residence time was found to increase with a decrease in impeller speed, decrease in flow rate, increase in bulk density and decrease in cohesion. The relative importance of input variables is shown using a VIP (Variable Importance Plot) in Fig. 7. Impeller speed and bulk density were found to be the two most important variables that affect mean residence time, whereas flow rate and cohesion were relatively less important.

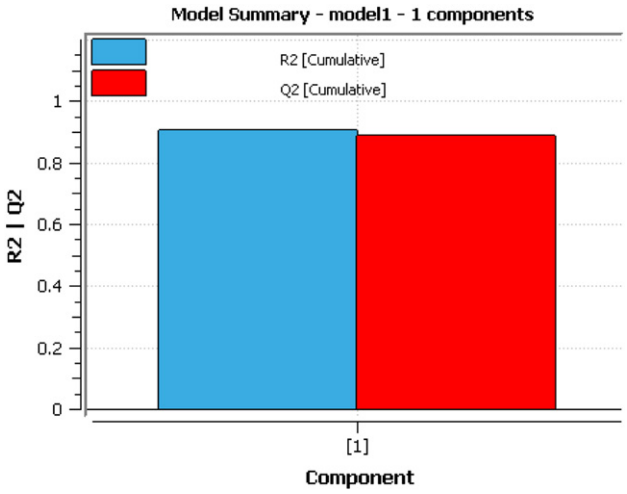

Fig. 5. PLS model for output variable — mean residence time.

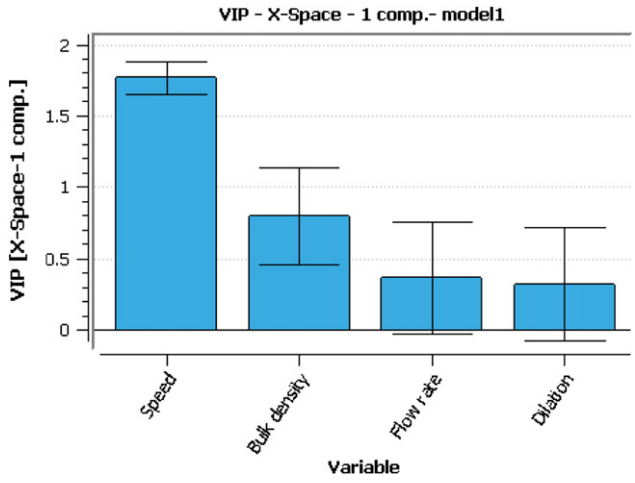

Fig. 7. Variable Importance Plot (VIP) of the PLS model of output variable — mean residence time.

Bulk density was found to be the key material property that affected mean residence time; cohesion did not show any clear trend. The relationship between bulk density and residence time is shown in Fig. 8. Increase in the bulk density leads to an increase in the mass hold-up in the continuous mixer, which increases residence time. This relationship is a strong function of impeller speed. At lower impeller speeds (40, 100 rpm) where the flow regime in the mixer is nearly quasi-static, the bulk density has a strong influence. At higher speeds (160, 250 rpm) the powder is fluidized in the mixer, and the bulk density has minimal effect on the residence time. At higher speeds, the forces exerted by the impeller exceed the gravitational settling forces.

As shown in Eq. (3), the number of blade passes experienced by the powder in the continuous mixer is a function of its residence time and rpm.

$$\#\text{Blade passes} = \text{Residence Time}\ (s) \times \frac{\text{Impeller Speed}\ (\text{rpm})}{60} \tag{3}$$

In our previous publication [1], it was shown that the number of blade passes greatly influence the mixing performance. As shown in Fig. 9, the number of blade passes goes through a maximum as the impeller speed increases. The optimum speed that provides a maximum number of blade passes is dependent on the relationship between residence time and impeller speed. It was observed that as the powder bulk density increases, the optimal speed decreases. As shown in Fig. 9, for Avicel® PH-101 and Avicel® PH-200 the optimal speed is ~160 rpm, whereas for Fast Flo lactose and dicalcium phosphate the optimal speed is ~100 rpm. This result can be used as a guideline to select optimal impeller speed based on the bulk density of the material.

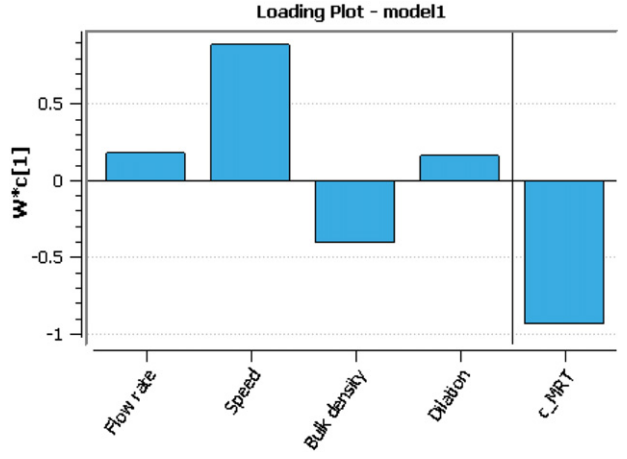

Fig. 6. Loading plot for the PLS model of output variable — mean residence time, and input variables — impeller speed, flow rate, bulk density and dilation.

4.1.3. Effect of material properties on the axial dispersion coefficient

The second important fitted parameter in the RTD model (Eq. (2)) is the axial dispersion coefficient. In our previous publication [11], the effect of process parameters (flow rate and impeller speed) on the axial dispersion coefficient was studied for the case of Avicel® PH-200. It was shown that while the axial dispersion coefficient increases with an increase in speed, the flow rate did not show a clear effect. In this case study, another PLS model was developed considering the axial dispersion coefficient as the output variable and the same set of input parameters (impeller speed, flow rate, bulk density and cohesion). As shown in the bar plot (Fig. 10), only 50% of the total

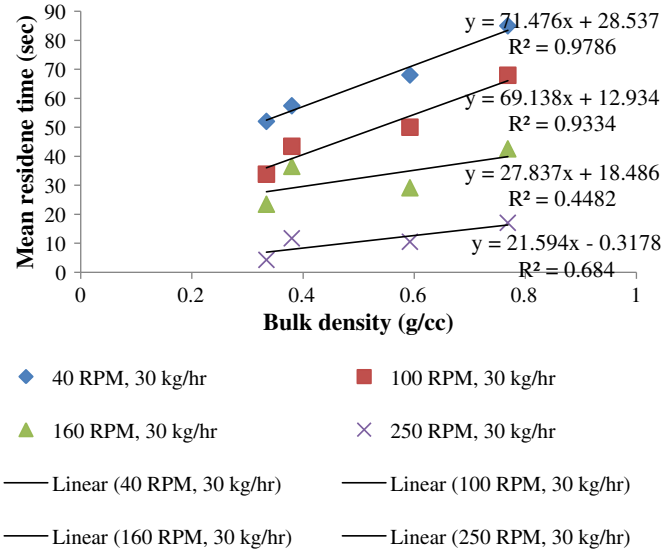

Fig. 8. Effect of bulk density on mean residence time at 30 kg/h.

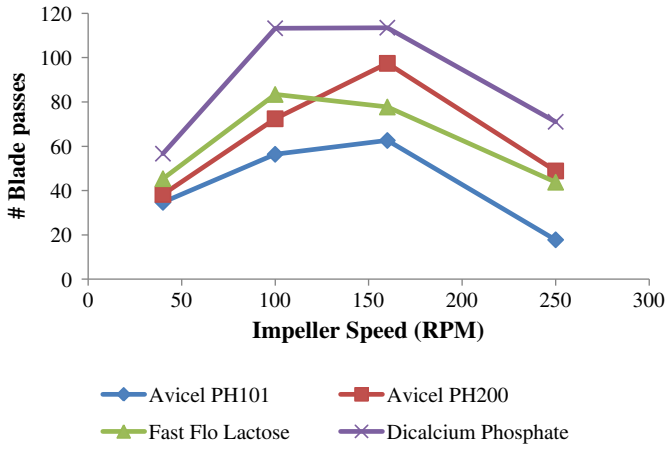

Fig. 9. Effect of impeller speed on the number of blade passes for different excipients.

variance was captured using this model. The relative trends between input and output variables are shown in Fig. 11. The axial dispersion coefficient was found to increase with an increase in speed, increase in dilation, decrease in bulk density, and increase in flow rate. The relative importance of input variables was analyzed by using a VIP plot. As shown in the VIP plot (Fig. 12), speed and cohesion were found to be the most important variables affecting the axial dispersion coefficient, and bulk density and flow rate had the least influence. In this DoE, bulk density did not show a clear effect on the axial dispersion coefficient because the variation in bulk density was primarily driven by the variation in true density (dicalcium phosphate = 2.31 g/cm^3, Lactose = 1.5 g/cm^3, MCC = 1.6 g/cm^3). If the materials have similar true densities, bulk density and cohesion are typically inversely related. However, for the materials in this study, the true densities are quite different, and the behavior of the bulk density is dominated by the true density. Since true density has essentially no effect on the axial dispersion coefficient, the effect of bulk density is not clearly observed either.

The relationship between dilation and axial dispersion coefficient is shown in Fig. 13. Speed and cohesion were found to interact significantly. At lower speeds (40, 100 rpm), cohesion did not affect axial dispersion coefficient; whereas at higher speeds (160, 250 rpm), higher cohesion leads to a higher axial dispersion coefficient. At higher speeds, the movement of powder is in the form of agglomerates as opposed to individual particles, which increases the magnitude of deviatory displacement steps of the powder "chunks" and essentially increases the axial dispersion coefficient.

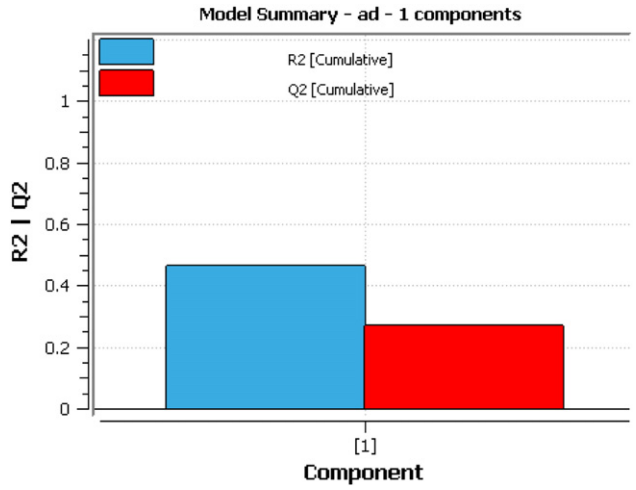

Fig. 10. PLS model for output variable — axial dispersion coefficient.

4.1.4. Predictive models suitable for process control

In our previous publication [11], a methodology was developed to predict blend uniformity (RSD) as a function of incoming feed rate variability and process parameters. As shown in Eq. (4), the total variance ($\sigma^2_{total,solid}$) in concentration observed at the mixer discharge can be decomposed as the variance due to incomplete axial mixing (σ^2_{fluid}) and the variance due to the non-ideal behavior of the powder mixing process ($\sigma^2_{ideal\_feed}$).

$$\sigma^2_{total,solid} = \sigma^2_{fluid} + \sigma^2_{ideal\_feed} \quad (4)$$

The variance due to the non-ideal powder mixing process can be due to several sources including incomplete transverse mixing, sample size, segregation, agglomeration, or a measurement method error. Usually this component of variance is empirical and needs to be characterized individually for each mixture. However the variability due to incomplete axial mixing can be computed by predicting the concentration of the output stream as a function of incoming concentrations and process parameters. The mathematical equation proposed by Danckwerts is provided in Eq. (5).

$$C_{out,fluid}(t) = \int_0^\infty C_{in}(t-\theta)E(\theta)d\theta \quad (5)$$

In order to use Eq. (5) as a predictive model for control purposes, a mathematical model for the RTD, and a separate empirical model for RTD parameters as a function of process parameters, are necessary. As described in the previous section, RTDs were modeled using FPEs (Eq. (2)). Empirical relationships were developed between RTD parameters (mean residence time (s), axial dispersion coefficient (cm^2/s)) and impeller speed (rpm). The model parameters and coefficient of correlation for each powder are listed in Tables 3 and 4. As shown in Table 3, a linear model worked reasonably well for predicting mean residence time as a function of impeller speed; and an exponential model showed the best possible fit for predicting the axial dispersion coefficient (Table 4).

4.2. Mixing effects in low shear (Gericke mixer) and high shear mixing (Quadro Comil) continuous mixing equipment

A case study on mixing of cohesive and free flowing powders in a continuous system was conducted. Micronized APAP and microcrystalline cellulose (MCC) were used as the model materials to represent cohesive and free flowing powders, respectively. The mixing problem in this case can be decomposed as a combination of macro-mixing and micro-mixing. Macro-mixing, which is governed by the bulk powder flow behavior in this mixer, is required to compensate for the incoming feed rate variability (axial mixing), and to mix the initially unmixed powders (radial mixing). Micro-mixing is also required to de-lump the agglomerates of acetaminophen and to reduce the scale of segregation. In this case study, effectiveness of Comil (Quadro) and a continuous mixer (Gericke) for micro and macro mixing was examined. Mixing experiments in individual units as well as integrated experiments were performed to optimize the overall mixing performance. The relative standard deviation (RSD) between the sample concentrations, as defined by Eq. (6), was used as the blend homogeneity index.

$$RSD = \frac{s}{\bar{C}} = \frac{\text{Standard deviation}}{\text{Average concentration}}, s = \sqrt{\frac{\sum_1^N \left(C_i - \bar{C}\right)^2}{N-1}} \quad (6)$$

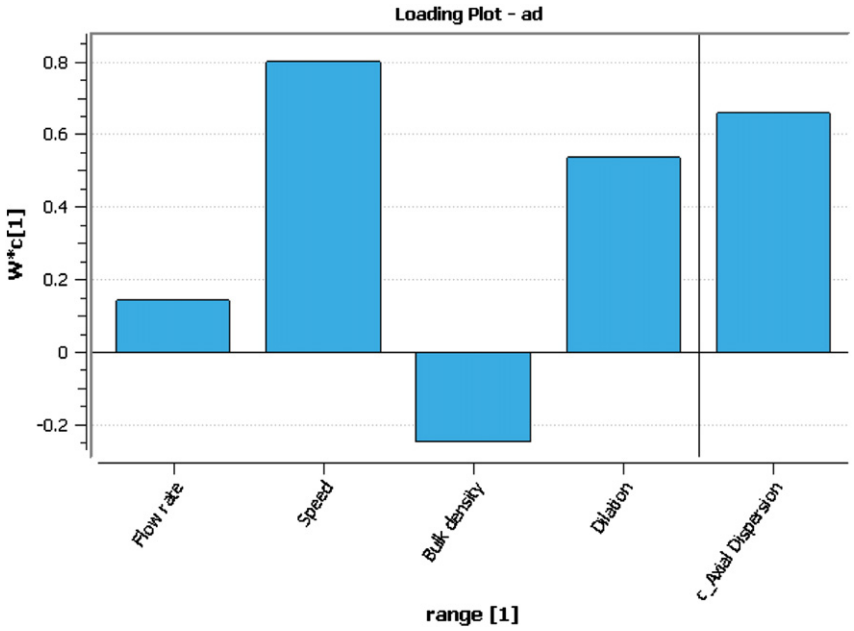

Fig. 11. Loading plot for the PLS model of output variable — axial dispersion coefficient, and input variables — impeller speed, flow rate, bulk density and dilation.

4.2.1. Low-shear mixing

The design of the impeller used in the Gericke continuous mixer is shown in Fig. 2(b). The paddle type impeller imposes axial and radial flow on the powder. The shear environment in this blender can be qualified as low-shear since the powder in the high shear zone (the region between the impeller tip and the mixer shell) is only a small fraction of the overall hold-up in the mixer, and the net movement of the powder is in the axial direction. The operational range of impeller speeds for this mixer lies between 0 and 300 rpm, which correspond to tip speeds in the range of 0–150 cm/s. Under lower impeller speeds (40–100 rpm), powder is relatively less fluidized in the mixer and its flow behavior can be described as a powder bed stirred by the impeller. Under these conditions, the axial velocities lie in the range of 0.6–1 cm/s, which indicates a low shear environment. Under higher impeller speeds (160–250 rpm), the powder bed is completely fluidized in the mixer which leads to fewer particle–particle contacts, which again imposes low shear on the powder.

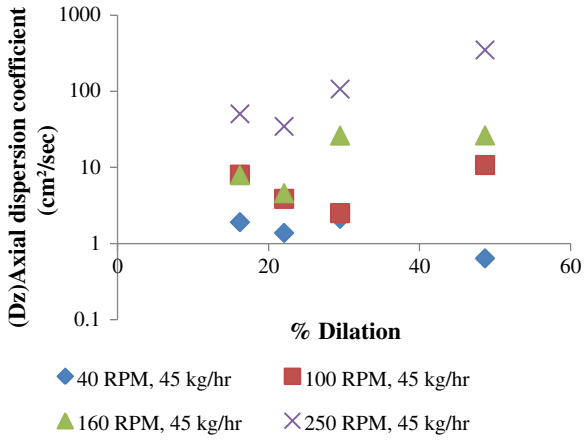

Fig. 13. Effect of dilation on axial dispersion coefficient.

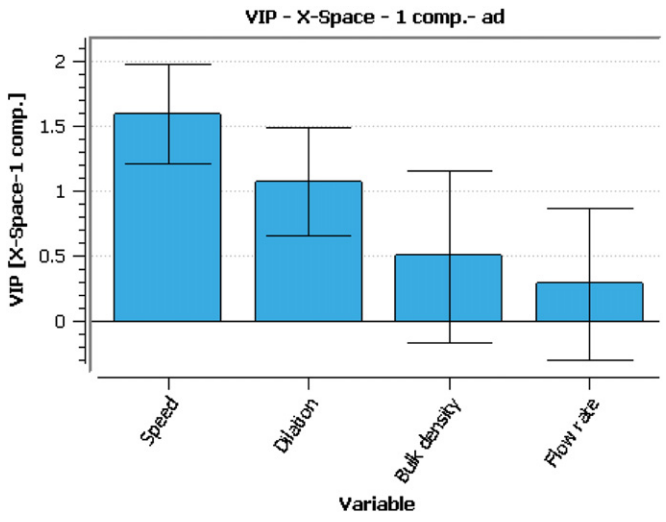

Fig. 12. Variable Importance Plot (VIP) for the PLS model of output variable — axial dispersion coefficient.

The effectiveness of the Gericke mixer for de-lumping and mixing was examined by mixing the two representative materials, micronized APAP and Avicel® PH-200 under 40, 160 and 250 rpm impeller speeds. While the process was operating under steady state, samples

Table 3
Predictive models for mean residence time (s).

Flow rate (kg/h)	Material	Model	Coeff. of correlation (R^2)
30	Avicel® PH-101	−0.2216 N + 58.868	0.989
30	Avicel® PH-200	−0.2113 N + 66.336	0.9795
30	Fast Flo lactose	−0.2772 N + 77.541	0.9872
30	Dicalcium phosphate	−0.3306 N + 98.599	0.9936
45	Avicel® PH-101	−0.155 N + 43.306	0.9442
45	Avicel® PH-200	−0.155 N + 50.248	0.8321
45	Fast Flo lactose	−0.2247 N + 61.848	0.9969
45	Dicalcium phosphate	−0.3232 N + 90.779	0.9955

Table 4
Predictive models for axial dispersion coefficient (cm^2/s).

Flow rate (kg/h)	Material	Model	Coeff. of correlation (R^2)
30	Avicel® PH-101	$0.444e^{0.0239.N}$	0.9778
30	Avicel® PH-200	$2.282e^{0.009.N}$	0.8362
30	Fast Flo lactose	$0.871e^{0.0116.N}$	0.9973
30	Dicalcium phosphate	$0.415e^{0.0208.N}$	0.9984
45	Avicel® PH-101	$0.314e^{0.0285.N}$	0.9664
45	Avicel® PH-200	$1.223e^{0.0144.N}$	0.9222
45	Fast Flo lactose	$0.7.27e^{0.0146.N}$	0.9383
45	Dicalcium phosphate	$0.667e^{0.0204.N}$	0.927

were extracted at the mixer discharge for assessing the blend uniformity. Samples were subsequently analyzed by NIR spectroscopy to determine the content of APAP. Mixing performance, measured as the RSD between concentrations of the extracted samples, is shown in Fig. 14 as a function of impeller speed. At the lowest speed (40 rpm), the worst mixing performance (RSD = 0.18) was obtained. With an increase in speed, RSD decreased to as low as ~0.10. As described in the previous section, the analytical method error in the NIR measurement is ~0.44. For the case of 10% APAP formulation, the inherent RSD for a well-mixed powder sample can be assumed to be ~0.04. Powder is considered to be well mixed if the RSD between the sample concentrations is close to the analytical method error. In this case since the minimum RSD obtained was almost twice the minimum possible RSD, the performance of the mixer was considered to be sub-optimal. Agglomerates of acetaminophen, visible to naked eyes, were observed in the powder samples. Incomplete de-lumping or micro-mixing was thus evident in this case. In order to identify the contribution of incomplete axial mixing, a simulation of axial mixing was performed using Eq. (5). A convolution algorithm was run in MATLAB using RTD datasets at 40, 160 and 250 rpm and the incoming feed rate datasets. Simulation results showed that the contribution of incomplete axial mixing to the variability in concentration at the mixer discharge was minimal. As described in the previous section, the radial mixing capability of the mixer is maximal under intermediate rotation rates. Given that the mixer was operated under optimal macro-mixing conditions (axial mixing and radial mixing), poor micro-mixing was identified as the primary source of mixing variability.

4.2.2. High shear mixing

The conical milling section and position of the impeller in the Comil is shown in Fig. 3(b). The impeller imposes a radial flow on the material which makes it pass through the screen. The Comil was operated at 1420 and 2280 rpm, which correspond to tip speeds of 802 and 1290 cm/s respectively. The extent of shear in the Comil is significantly greater than the Gericke mixer since the material has to pass through the high shear zone before it exits the mill. The schematics of the experimental set-up for conducting mixing studies in the Comil is illustrated in Fig. 15(a). A full factorial DoE with two levels of impeller speed (1420 rpm, 2280 rpm) and two screen sizes (600, 800 μm) was conducted. Since the main function of the Comil in this case study is de-lumping and not size reduction, the screen size was chosen such that the hole diameter is significantly greater than the d90 of the particle size distribution of the powder blend (d90 = ~400 μm).

Continuous mixing in the Comil was facilitated by feeding individual powders using the same feed setting as used for the Gericke mixer. As shown in Fig. 15(b), lower impeller speeds and smaller screens lead to better mixing performance. Quantitatively, the effect of screen size was less than the effect of speed. The presence of a screen significantly reduced agglomerates in the powder blend. Smaller error bars in the RSD measurement is also an indication of reduced number of agglomerates in the powder blend. However, RSD values

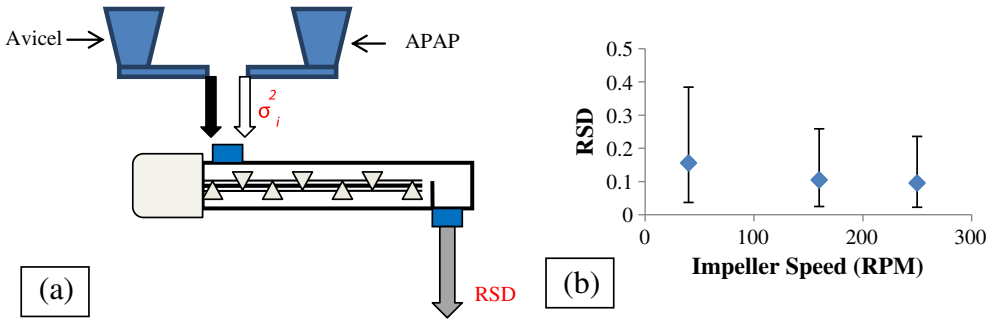

Fig. 14. (a) Schematics of the experimental set-up for mixing in Gericke continuous mixer. (b) Effect of impeller speed on blend uniformity (RSD).

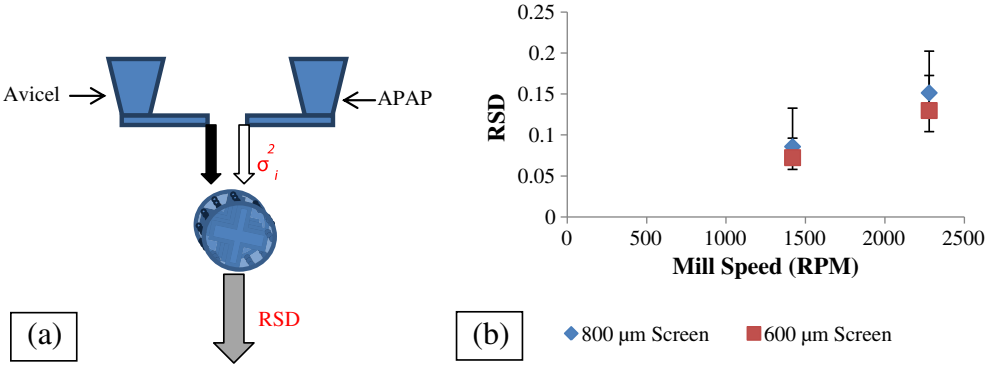

Fig. 15. (a) Schematics of the experimental set-up for mixing in Comil. (b) Effect of impeller speed and screen size on blend uniformity (RSD).

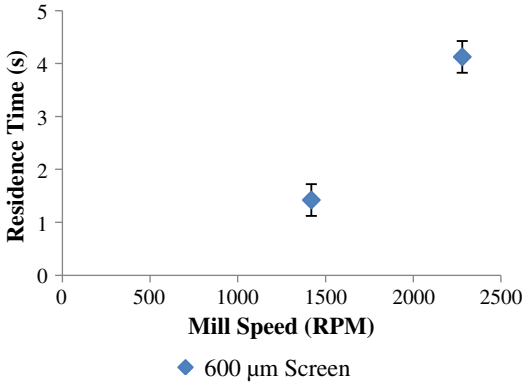

Fig. 16. Effect of mill speed on residence time.

obtained over the operating range of the mill (0.08–0.15) were greater than the analytical method error (RSD = 0.04), and mixing performance again was considered to be sub-optimal. In this case, the de-lumping/micro-mixing behavior was better than the Gericke mixer, poor macro-mixing was identified as the potential source of mixing variability.

In order to qualify the macro-mixing capability of the Comil, the residence time of the powder in the mill was measured. Residence time was measured by monitoring the steady-state powder hold-up in the continuous mixer. As shown in Fig. 16, residence time in the mill increase from 1.4 s to 4.2 s as the impeller speed increases. This trend indicates that with an increase in speed, stagnation of the material in the mill increases, possibly near the closed area of the screen. The fact that an increase in residence time in the mill does not necessarily decrease RSD clearly indicates that under high speeds there is a possibility of short-circuiting of the material. Very low mill speeds (<1400 rpm) were not used since the de-lumping efficiency of the mill is adversely affected at lower speeds, and there is a possibility of preferential stagnation in the mill.

4.2.3. Integrated low shear mixing — de-lumping process

Mixing experiments performed in individual units led to the conclusion that it was difficult to achieve good blend uniformity using either of the individual pieces of equipment selected for this study. Mixing experiments were then performed in an integrated fashion which included two scenarios, namely 'low-shear mixing first' and 'high-shear mixing first'. In this set of experiments, process parameters of only the first unit were varied; the second unit was operated only under the optimal (best) operating condition.

4.2.3.1. Low-shear mixing first. The schematics of the experimental set-up for the first scenario is shown in Fig. 17(a). Impeller speed of the Gericke mixer was varied from 40 to 250 rpm; the Comil was operated at a constant speed of 1420 rpm. As shown in Fig. 17(b), RSD values slightly decreased after the milling stage. However RSD values were still higher than the minimum possible RSD. These results indicate that further mixing is necessary. The Comil essentially de-lumps the remaining agglomerates from the incoming powder stream which creates high concentrations of APAP locally. There needs to be another mixing stage to mix the de-lumped APAP uniformly with the rest of the powder. In this scenario, since a post-low-shear mixing stage is missing, overall mixing performance remains sub-optimal.

4.2.3.2. High-shear mixing first. The schematics of the experimental set-up for the second scenario is shown in Fig. 18(a). In this case, speed of the Comil was varied from 1420 to 2280 rpm, and the Gericke mixer was operated only at 160 rpm. Mixing performance showed significant improvement after the second mixing stage; RSD values being lower than the analytical method error indicates that the best measurable mixing performance has been achieved (or nearly achieved). A separate mixing experiment was performed by mixing the initially de-lumped material in a batch blender. De-lumped powder was blended for 30 min in an '8 Quart V-blender' operating at 12.5 shell rpm. Batch mixing showed similar degree of mixing performance; RSDs in the range of 0.02–0.04 were obtained. Since RSD values obtained after the batch mixing step were close to the analytical method error, further mixing is not required.

5. Conclusions

In the first part of this paper, the role of bulk material properties on the powder flow behavior in the continuous mixer was identified. In the second part, an integrated continuous low and high shear mixing strategy suitable for mixing cohesive materials was presented.

Relative trends between input variables (impeller speed, flow rate, bulk density and cohesion) and output variables (mean residence time and axial dispersion coefficient) were identified by building a PLS model. In this case study, bulk density was found to be the key material property that affects mean residence time; cohesion did not show a clear effect. The effect of cohesion was not seen because the true densities of the materials included in the DoE were significantly different. The effect of cohesion needs to be studied using

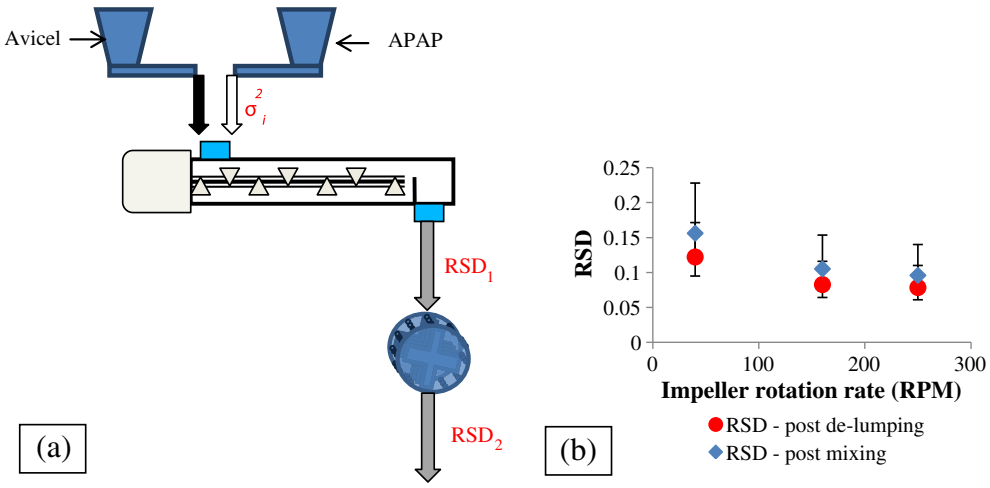

Fig. 17. (a) Schematics of the experimental set-up for integrated low and high shear mixing (low-shear mixing first). (b) Mixing performance after low and high shear mixing.

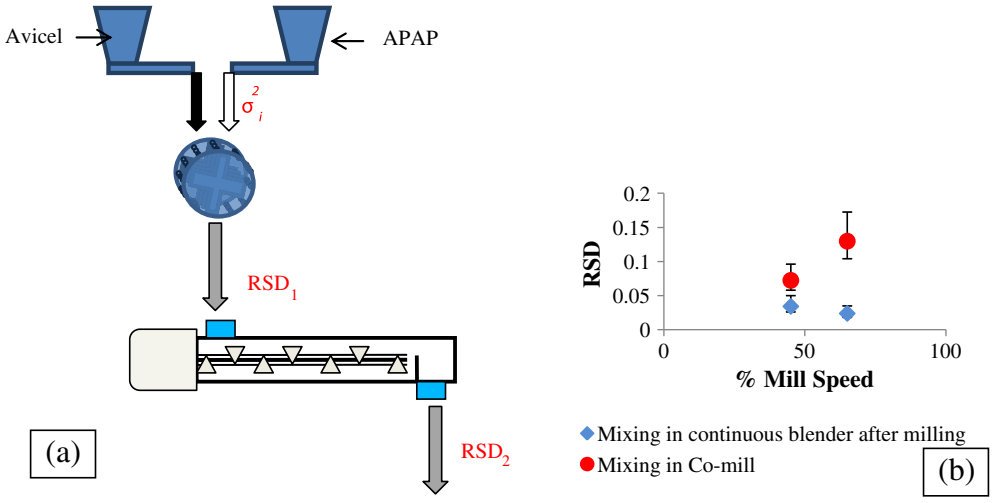

Fig. 18. (a) Schematics of the experimental set-up for integrated low and high shear mixing (high-shear mixing first). (b) Mixing performance after high and low shear mixing.

materials of nearly equal true densities, either by varying the particle size or adding minor ingredients which affect cohesion. The relationship between the number of blade passes and impeller speed was characterized for different materials. The optimal speed, which exhibits the highest number of blade passes, was found to be lower for materials with greater bulk densities. This result provides a design rule for selecting impeller speed based on the material bulk density. On the other hand, axial dispersion coefficient was affected by cohesion (or dilation), and not the bulk density of the material. Cohesion and impeller speed showed a significant interaction. At lower impeller speeds, cohesion hardly affected axial dispersion coefficient, however at higher impeller speeds, greater cohesion leads to higher axial dispersion coefficients.

Mixing behavior in a low shear mixer (Gericke) and a high shear Comil (Quadro) was examined. The Gericke mixer was found to be a poor micro-mixer/de-lumper, whereas the Comil was found to be a good micro-mixer and poor macro-mixer. Short-circuiting of materials was identified to be main source of poor macro-mixing in the Comil. Macro-mixing capability of the Gericke mixer and micro-mixing capability of the Comil was utilized by integrating them together. Integrated system with high shear mixing first provided the best possible mixing performance.

Acknowledgments

This work was supported by NSF grant to ERC-SOPS (Engineering Research Center for Structured Organic Particulate Systems).

References

[1] A.U. Vanarase, F.J. Muzzio, Effect of operating conditions and design parameters in a continuous powder mixer, Powder Technology 208 (2011) 26–36.
[2] P.M. Portillo, A.U. Vanarase, A. Ingram, J.K. Seville, M.G. Ierapetritou, F.J. Muzzio, Investigation of the effect of impeller rotation rate, powder flow rate, and cohesion on powder flow behavior in a continuous blender using PEPT, Chemical Engineering Science 65 (2010) 5658–5668.
[3] P.M. Portillo, M.G. Ierapetritou, F.J. Muzzio, Characterization of continuous convective powder mixing processes, Powder Technology 182 (2008) 368–378.
[4] H. Berthiaux, K. Marikh, C. Gatumel, Continuous mixing of powder mixtures with pharmaceutical process constraints, Chemical Engineering and Processing: Process Intensification 47 (2008) 2315–2322.
[5] A. Dubey, A. Sarkar, M. Ierapetritou, C.R. Wassgren, F.J. Muzzio, Computational approaches for studying the granular dynamics of continuous blending processes, 1—DEM based methods, Macromolecular Materials and Engineering 296 (2011) 290–307.
[6] P.V. Danckwerts, Continuous flow systems. Distribution of residence times, Chemical Engineering Science 2 (1953) 1–13.
[7] V. Kehlenbeck, K. Sommer, Modeling of the mixing process of very fine powders in a continuous dynamic mixer, Fourth International Conference on Conveying and Handling of Particulate Solids, 9, 2003, pp. 26–31.
[8] R.G. Sherritt, J. Chaouki, A.K. Mehrotra, L.A. Behie, Axial dispersion in the three-dimensional mixing of particles in a rotating drum reactor, Chemical Engineering Science 58 (2003) 401–415.
[9] K. Marikh, H. Berthiaux, V. Mizonov, E. Barantseva, D. Ponomarev, Flow analysis and Markov chain modelling to quantify the agitation effect in a continuous powder mixer, Chemical Engineering Research and Design 84 (2006) 1059–1074.
[10] G.R. Ziegler, C.A. Aguilar, Residence time distribution in a co-rotating, twin-screw continuous mixer by the step change method, Journal of Food Engineering 59 (2003) 161–167.
[11] Y. Gao, A. Vanarase, F. Muzzio, M. Ierapetritou, Characterizing continuous powder mixing using residence time distribution, Chemical Engineering Science 66 (2011) 417–425.
[12] P. Begat, D.A.V. Morton, J.N. Staniforth, R. Price, The cohesive–adhesive balances in dry powder inhaler formulations I: direct quantification by atomic force microscopy, Pharmaceutical Research 21 (2004) 1591–1597.
[13] M. Llusa, K. Sturm, O. Sudah, H. Stamato, D.J. Goldfarb, H. Ramachandruni, et al., Effect of high shear blending protocols and blender parameters on the degree of API agglomeration in solid formulations, Industrial and Engineering Chemistry Research 48 (2009) 93–101.
[14] A. Faqih, B. Chaudhuri, A.W. Alexander, C. Davies, F.J. Muzzio, M. Silvina Tomassone, An experimental/computational approach for examining unconfined cohesive powder flow, International Journal of Pharmaceutics 324 (2006) 116–127.